

4 Scattering by particles on or near a plane surface

Adrian Doicu, Roman Schuh and Thomas Wriedt

4.1 Introduction

Computation of light scattering from particles deposited upon a surface is of great interest in the simulation, development and calibration of surface scanners for wafer inspection [1]. More recent applications include laser cleaning [2], scanning near-field optical microscopy (SNOM) [3] and plasmon resonances effects in surface-enhanced Raman spectroscopy (SERS) [4]. Several studies have addressed this scattering problem using different methods. Simplified theoretical models have been developed on the basis of Lorenz–Mie theory and Fresnel surface reflection [5–8]. A coupled-dipole algorithm has been employed by Taubenblatt and Tran [9] and Nebeker *et al.* [10] using a three-dimensional array of dipoles to model a feature shape and the Sommerfeld integrals to describe the interaction between a dipole and a surface. The theoretical aspects of the coupled-dipole model has been fully outlined by R. Schmehl [11]. A model based on the discrete source method has been given by Eremin and Orlov [12, 13], whereas the transmission conditions at the interface are satisfied analytically and the fields of discrete sources are derived by using the Green tensor for a plane surface. More details on computational methods and experimental results can be found in a book edited by Moreno and Gonzales [14].

Similar scattering problems have been solved by Kristensson and Ström [15], and Hackmann and Sammelmann [16] in the framework of the null-field method. Acoustic scattering from a buried inhomogeneity has been considered by Kristensson and Ström on the assumption that the free-field \mathbf{T} -matrix of the particle modifies the free-field \mathbf{T} -operator of the arbitrary surface. By projecting the free-field \mathbf{T} -operator of the surface onto a spherical basis, an infinite system of linear equations for the free-field \mathbf{T} -matrix of the particle has been derived. In contrast, Hackmann and Sammelmann assumed that the free-field \mathbf{T} -operator of the surface modifies the free-field \mathbf{T} -matrix of the particle, and in this case, the free-field \mathbf{T} -matrix of the particle has been projected onto a rectangular basis and an integral equation for the spectral amplitudes of the fields has been obtained.

More recently Mackowski [24] extended the \mathbf{T} -matrix approach to multiple spheres on a plane interface.

In this contribution we use the null-field method to analyze the scattering by particles on a plane surface. Our intention is to treat several scattering geometries which occur in practice. These include the scattering by single particles on a plane surface or on a plane surface coated with a film, and the scattering by systems of particles.

4.1.1 Single particle on or near a plane surface

In this section we extend the results of Bobbert and Vlieger [5] to the case of axisymmetric particles situated on or near a plane surface. The scattering problem is a multiple particles problem and the solution method is the separation of variables technique. To model the scattering problem in the framework of the separation of variables technique one must address how the radiation interacts with the particle. The incident field strikes the particle either directly or after interacting with the surface, while the fields emanating from the particle may also reflect off the surface and interact with the particle again. The transition matrix relating the incident and scattered field coefficients is computed in the framework of the null-field method and the reflection matrix characterizing the reflection of the scattered field by the surface is computed by using the integral representation for the vector spherical wave functions.

The geometry of the scattering problem is shown in Fig. 4.1. An axisymmetric particle is situated in the neighborhood of a plane surface Σ , so that its axis of symmetry is normal to the plane surface. The z -axis of the particle coordinate system $Oxyz$ is directed along the axis of symmetry and the origin O is situated at the distance z_0 below the plane surface. The incident radiation is a linearly polarized vector plane wave propagating in the ambient medium (the medium below the surface Σ)

$$\mathbf{E}_e(\mathbf{r}) = (E_{e0,\beta}\mathbf{e}_\beta + E_{e0,\alpha}\mathbf{e}_\alpha) e^{i\mathbf{k}_e \cdot \mathbf{r}}, \quad (4.1)$$

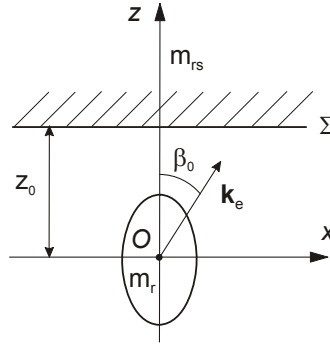


Fig. 4.1. Geometry of an axisymmetric particle situated near a plane surface. The external excitation is a vector plane wave propagating in the ambient medium.

and the wave vector \mathbf{k}_e , $\mathbf{k}_e = k_s \mathbf{e}_k$, is assumed to be in the xz -plane and to enclose the angle β_0 with the z -axis.

The incident wave strikes the particle either directly or after interacting with the surface. The direct and the reflected incident fields are expanded in terms of regular vector spherical wave functions

$$\mathbf{E}_e(\mathbf{r}) = \sum_{n_1=1}^{\infty} \sum_{m=-n_1}^{n_1} a_{mn_1}^0 \mathbf{M}_{mn_1}^1(k_s \mathbf{r}) + b_{mn_1}^0 \mathbf{N}_{mn_1}^1(k_s \mathbf{r}) \quad (4.2)$$

and

$$\mathbf{E}_e^R(\mathbf{r}) = \sum_{n_1=1}^{\infty} \sum_{m=-n_1}^{n_1} a_{mn_1}^R \mathbf{M}_{mn_1}^1(k_s \mathbf{r}) + b_{mn_1}^R \mathbf{N}_{mn_1}^1(k_s \mathbf{r}), \quad (4.3)$$

respectively, and we define the total expansion coefficients a_{mn_1} and b_{mn_1} by the relations

$$\begin{aligned} a_{mn_1} &= a_{mn_1}^0 + a_{mn_1}^R, \\ b_{mn_1} &= b_{mn_1}^0 + b_{mn_1}^R. \end{aligned}$$

The coefficients $a_{mn_1}^0$ and $b_{mn_1}^0$ are the expansion coefficients of a vector plane wave travelling in the $(\beta_0, 0)$ direction,

$$\begin{aligned} a_{mn_1}^0 &= -\frac{4j^{n_1}}{\sqrt{2n_1(n_1+1)}} \left[jm\pi_{n_1}^{|m|}(\beta_0) E_{e0,\beta} + \tau_{n_1}^{|m|}(\beta_0) E_{e0,\alpha} \right], \\ b_{mn_1}^0 &= -\frac{4j^{n_1+1}}{\sqrt{2n_1(n_1+1)}} \left[\tau_{n_1}^{|m|}(\beta_0) E_{e0,\beta} - jm\pi_{n_1}^{|m|}(\beta_0) E_{e0,\alpha} \right], \end{aligned}$$

while the coefficients $a_{mn_1}^R$ and $b_{mn_1}^R$ are the expansion coefficients of a vector plane wave travelling in the $(\pi - \beta_0, 0)$ direction. The part of the incident field that reflects off the surface will undergo a Fresnel reflection and it will be out of phase by an amount of $\exp(2jk_s z_0 \cos \beta_0)$. This phase factor arises from the phase difference between the plane wave and its reflected wave in O . The resulting expressions for $a_{mn_1}^R$ and $b_{mn_1}^R$ are

$$\begin{aligned} a_{mn_1}^R &= -\frac{4j^{n_1}}{\sqrt{2n_1(n_1+1)}} \left[jm\pi_{n_1}^{|m|}(\pi - \beta_0) E_{e0,\beta}^R + \tau_{n_1}^{|m|}(\pi - \beta_0) E_{e0,\alpha}^R \right], \\ b_{mn_1}^R &= -\frac{4j^{n_1+1}}{\sqrt{2n_1(n_1+1)}} \left[\tau_{n_1}^{|m|}(\pi - \beta_0) E_{e0,\beta}^R - jm\pi_{n_1}^{|m|}(\pi - \beta_0) E_{e0,\alpha}^R \right], \end{aligned}$$

where

$$\begin{aligned} E_{e0,\beta}^R &= r_{\parallel}(\beta_0) e^{2jk_s z_0 \cos \beta_0} E_{e0,\beta}, \\ E_{e0,\alpha}^R &= r_{\perp}(\beta_0) e^{2jk_s z_0 \cos \beta_0} E_{e0,\alpha}, \end{aligned}$$

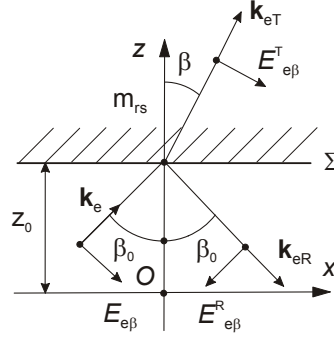


Fig. 4.2. Reflection and refraction of a vector plane wave (propagating in the ambient medium) at the interface Σ .

with $r_{\parallel}(\beta_0)$ and $r_{\perp}(\beta_0)$ being the Fresnel reflection coefficients for parallel and perpendicular polarizations, respectively. The Fresnel reflection coefficients are given by

$$r_{\parallel}(\beta_0) = \frac{m_{rs} \cos \beta_0 - \cos \beta}{m_{rs} \cos \beta_0 + \cos \beta},$$

$$r_{\perp}(\beta_0) = \frac{\cos \beta_0 - m_{rs} \cos \beta}{\cos \beta_0 + m_{rs} \cos \beta},$$

where m_{rs} is the relative refractive index of the substrate with respect to the ambient medium and β is the angle of refraction (Fig. 4.2). The angles of incidence and refraction are related to each other by Snell's law,

$$\sin \beta = \frac{1}{m_{rs}} \sin \beta_0,$$

$$\cos \beta = \pm \sqrt{1 - \sin^2 \beta},$$

and for real values of m_{rs} , the sign of the square root is plus, while for complex values of m_{rs} , the sign of the square root is chosen such that $\text{Im}\{m_{rs} \cos \beta\} > 0$. This choice guarantees that the amplitude of the refracted wave propagating in the positive direction of the z -axis would tend to zero with increasing distance z .

The scattered field is expanded in terms of radiating vector spherical wave functions

$$\mathbf{E}_s(\mathbf{r}) = \sum_{n=1}^{\infty} \sum_{m=-n}^n f_{mn} \mathbf{M}_{mn}^3(k_s \mathbf{r}) + g_{mn} \mathbf{N}_{mn}^3(k_s \mathbf{r}), \quad (4.4)$$

and the rest of our analysis concerns the calculation of the expansion coefficients f_{mn} and g_{mn} . In addition to the fields described by (4.2)–(4.4), a fourth field exists in the ambient medium. This field is a result of the scattered field reflecting off the surface and striking the particle. It can be expressed as

$$\mathbf{E}_s^R(\mathbf{r}) = \sum_{n=1}^{\infty} \sum_{m=-n}^n f_{mn} \mathbf{M}_{mn}^{3,R}(k_s \mathbf{r}) + g_{mn} \mathbf{N}_{mn}^{3,R}(k_s \mathbf{r}), \quad (4.5)$$

where $\mathbf{M}_{mn}^{3,R}(k_s \mathbf{r})$ and $\mathbf{N}_{mn}^{3,R}(k_s \mathbf{r})$ are the radiating vector spherical wave functions reflected by the surface. Accordingly to Videen [6–8], the field \mathbf{E}_s^R will be designated as the interacting field. For \mathbf{r} inside a sphere enclosed in the particle and a given azimuthal mode m , we anticipate an expansion of the reflected vector spherical wave functions of the form

$$\begin{pmatrix} \mathbf{M}_{mn}^{3,R}(k_s \mathbf{r}) \\ \mathbf{N}_{mn}^{3,R}(k_s \mathbf{r}) \end{pmatrix} = \sum_{n_1=1}^{\infty} \begin{pmatrix} \alpha_{mnn_1} \\ \gamma_{mnn_1} \end{pmatrix} \mathbf{M}_{mn_1}^1(k_s \mathbf{r}) + \begin{pmatrix} \beta_{mnn_1} \\ \delta_{mnn_1} \end{pmatrix} \mathbf{N}_{mn_1}^1(k_s \mathbf{r}). \quad (4.6)$$

Inserting (4.6) into (4.5), we derive a series representation for the interacting field in terms of regular vector spherical wave functions,

$$\mathbf{E}_s^R(\mathbf{r}) = \sum_{n_1=1}^{\infty} \sum_{m=-n_1}^{n_1} [f_{mn_1}^R \mathbf{M}_{mn_1}^1(k_s \mathbf{r}) + g_{mn_1}^R \mathbf{N}_{mn_1}^1(k_s \mathbf{r})], \quad (4.7)$$

where

$$\begin{pmatrix} f_{mn_1}^R \\ g_{mn_1}^R \end{pmatrix} = \sum_{n=1}^{\infty} \begin{pmatrix} \alpha_{mnn_1} \\ \beta_{mnn_1} \end{pmatrix} f_{mn} + \begin{pmatrix} \gamma_{mnn_1} \\ \delta_{mnn_1} \end{pmatrix} g_{mn}. \quad (4.8)$$

In the null-field method, the scattered field coefficients are related to the expansion coefficients of the fields striking the particle by the transition matrix \mathbf{T} . For an axisymmetric particle, the equations become uncoupled, permitting a separate solution for each azimuthal mode. Thus, for a fixed azimuthal mode m , we truncate the expansions given by (4.2)–(4.4) and (4.7), and derive the following matrix equation:

$$\begin{bmatrix} f_{mn} \\ g_{mn} \end{bmatrix} = [T_{mn, mn_1}] \left(\begin{bmatrix} a_{mn_1} \\ b_{mn_1} \end{bmatrix} + \begin{bmatrix} f_{mn_1}^R \\ g_{mn_1}^R \end{bmatrix} \right), \quad (4.9)$$

where n and n_1 ranges from 1 to N_{rank} , and m ranges from $-M_{\text{rank}}$ to M_{rank} , with N_{rank} and M_{rank} being the maximum expansion and azimuthal orders, respectively. The expansion coefficients of the interacting field are related to the scattered field coefficients by a so-called reflection matrix:

$$\begin{bmatrix} f_{mn_1}^R \\ g_{mn_1}^R \end{bmatrix} = [A_{mn_1 n}] \begin{bmatrix} f_{mn} \\ g_{mn} \end{bmatrix}, \quad (4.10)$$

where, in view of (4.8),

$$[A_{mn_1 n}] = \begin{bmatrix} \alpha_{mnn_1} & \gamma_{mnn_1} \\ \beta_{mnn_1} & \delta_{mnn_1} \end{bmatrix}.$$

Now it is apparent that the scattered field coefficients f_{mn} and g_{mn} can be obtained by combining the matrix equations (4.9) and (4.10), and the result is [17]

$$(\mathbf{I} - [T_{mn, mn_1}][A_{mn_1 n}]) \begin{bmatrix} f_{mn} \\ g_{mn} \end{bmatrix} = [T_{mn, mn_1}] \begin{bmatrix} a_{mn_1} \\ b_{mn_1} \end{bmatrix}. \quad (4.11)$$

To derive the expression of the reflection matrix we use the integral representations for the radiating vector spherical wave functions,

$$\begin{pmatrix} \mathbf{M}_{mn}^3(k_s \mathbf{r}) \\ \mathbf{N}_{mn}^3(k_s \mathbf{r}) \end{pmatrix} = -\frac{1}{2\pi j^{n+1}} \frac{1}{\sqrt{2n(n+1)}} \int_0^{2\pi} \int_0^{\pi/2-j\infty} \begin{bmatrix} m\pi_n^{|m|}(\beta) \\ \tau_n^{|m|}(\beta) \end{bmatrix} \mathbf{e}_\beta \\ + j \begin{bmatrix} \tau_n^{|m|}(\beta) \\ m\pi_n^{|m|}(\beta) \end{bmatrix} \mathbf{e}_\alpha \Big] e^{jm\alpha} e^{j\mathbf{k}(\beta, \alpha) \cdot \mathbf{r}} \sin \beta \, d\beta \, d\alpha, \quad (4.12)$$

where (k_s, β, α) are the spherical coordinates of the wave vector \mathbf{k} , and $(\mathbf{e}_k, \mathbf{e}_\beta, \mathbf{e}_\alpha)$ are the spherical unit vectors of \mathbf{k} . Each reflected plane wave in (4.12) will contain a Fresnel reflection term and a phase term equivalent to $\exp(2jk_s z_0 \cos \beta)$. The reflected vector spherical wave functions can be expressed as

$$\begin{pmatrix} \mathbf{M}_{mn}^{3,R}(k_s \mathbf{r}) \\ \mathbf{N}_{mn}^{3,R}(k_s \mathbf{r}) \end{pmatrix} = -\frac{1}{2\pi j^{n+1}} \frac{1}{\sqrt{2n(n+1)}} \int_0^{2\pi} \int_0^{\pi/2-j\infty} \begin{bmatrix} m\pi_n^{|m|}(\beta) \\ \tau_n^{|m|}(\beta) \end{bmatrix} r_{\parallel}(\beta) \mathbf{e}_{\beta R} \\ + j \begin{bmatrix} \tau_n^{|m|}(\beta) \\ m\pi_n^{|m|}(\beta) \end{bmatrix} r_{\perp}(\beta) \mathbf{e}_{\alpha R} \Big] e^{jm\alpha} e^{2jk_s z_0 \cos \beta} e^{j\mathbf{k}_R(\beta_R, \alpha_R) \cdot \mathbf{r}} \\ \times \sin \beta \, d\beta \, d\alpha,$$

where $\beta_R = \pi - \beta$, $\alpha_R = \alpha$, (k_s, β_R, α_R) are the spherical coordinates of the reflected wave vector \mathbf{k}_R , and $(\mathbf{e}_{k_R}, \mathbf{e}_{\beta_R}, \mathbf{e}_{\alpha_R})$ are the spherical unit vectors of \mathbf{k}_R . For \mathbf{r} inside a sphere enclosed in the particle, we expand each plane wave in terms of regular vector spherical wave functions

$$\begin{pmatrix} \mathbf{e}_{\beta R} \\ \mathbf{e}_{\alpha R} \end{pmatrix} e^{j\mathbf{k}_R \cdot \mathbf{r}} = -\sum_{n_1=1}^{\infty} \sum_{m_1=-n_1}^{n_1} \frac{4j^{n_1}}{\sqrt{2n_1(n_1+1)}} \begin{bmatrix} jm_1 \pi_{n_1}^{|m_1|}(\pi - \beta) \\ \tau_{n_1}^{|m_1|}(\pi - \beta) \end{bmatrix} \\ \times \mathbf{M}_{m_1 n_1}^1(k_s \mathbf{r}) + \begin{bmatrix} j\tau_{n_1}^{|m_1|}(\pi - \beta) \\ m_1 \pi_{n_1}^{|m_1|}(\pi - \beta) \end{bmatrix} \mathbf{N}_{m_1 n_1}^1(k_s \mathbf{r}) \Big] e^{-jm_1 \alpha},$$

and obtain the following expressions for the elements of the reflection matrix:

$$\alpha_{mnn_1} = \frac{2j^{n_1-n}}{\sqrt{nn_1(n+1)(n_1+1)}} \int_0^{\pi/2-j\infty} \left[m^2 \pi_n^{|m|}(\beta) \pi_{n_1}^{|m|}(\pi - \beta) r_{\parallel}(\beta) \right. \\ \left. + \tau_n^{|m|}(\beta) \tau_{n_1}^{|m|}(\pi - \beta) r_{\perp}(\beta) \right] e^{2jk_s z_0 \cos \beta} \sin \beta \, d\beta, \quad (4.13)$$

$$\begin{aligned} \beta_{mnn_1} &= \frac{2j^{n_1-n}}{\sqrt{nn_1(n+1)(n_1+1)}} \int_0^{\pi/2-j\infty} m \left[\pi_n^{(|m|)}(\beta) \tau_{n_1}^{(|m|)}(\pi-\beta) r_{\parallel}(\beta) \right. \\ &\quad \left. + \tau_n^{(|m|)}(\beta) \pi_{n_1}^{(|m|)}(\pi-\beta) r_{\perp}(\beta) \right] e^{2jk_s z_0 \cos \beta} \sin \beta \, d\beta, \end{aligned} \quad (4.14)$$

$$\begin{aligned} \gamma_{mnn_1} &= \frac{2j^{n_1-n}}{\sqrt{nn_1(n+1)(n_1+1)}} \int_0^{\pi/2-j\infty} m \left[\tau_n^{(|m|)}(\beta) \pi_{n_1}^{(|m|)}(\pi-\beta) r_{\parallel}(\beta) \right. \\ &\quad \left. + \pi_n^{(|m|)}(\beta) \tau_{n_1}^{(|m|)}(\pi-\beta) r_{\perp}(\beta) \right] e^{2jk_s z_0 \cos \beta} \sin \beta \, d\beta, \end{aligned} \quad (4.15)$$

$$\begin{aligned} \delta_{mnn_1} &= \frac{2j^{n_1-n}}{\sqrt{nn_1(n+1)(n_1+1)}} \int_0^{\pi/2-j\infty} \left[\tau_n^{(|m|)}(\beta) \tau_{n_1}^{(|m|)}(\pi-\beta) r_{\parallel}(\beta) \right. \\ &\quad \left. + m^2 \pi_n^{(|m|)}(\beta) \pi_{n_1}^{(|m|)}(\pi-\beta) r_{\perp}(\beta) \right] e^{2jk_s z_0 \cos \beta} \sin \beta \, d\beta, \end{aligned} \quad (4.16)$$

An approximate expression for the reflection matrix can be derived if we assume that the interacting radiation strikes the surface at normal incidence. Assuming $r(0) = r_{\perp}(\beta) = -r_{\parallel}(\beta)$, changing the variable from β to $\beta_R = \pi - \beta$, and using the relations

$$\begin{aligned} \pi_n^{(|m|)}(\pi - \beta_R) &= (-1)^{n-|m|} \pi_n^{(|m|)}(\beta_R), \\ \tau_n^{(|m|)}(\pi - \beta_R) &= (-1)^{n-|m|+1} \tau_n^{(|m|)}(\beta_R), \end{aligned}$$

yields the following simplified integral representations for the reflected vector spherical wave functions:

$$\begin{aligned} \begin{pmatrix} \mathbf{M}_{mn}^{3,R}(k_s \mathbf{r}) \\ \mathbf{N}_{mn}^{3,R}(k_s \mathbf{r}) \end{pmatrix} &= -\frac{(-1)^{n-|m|} r(0)}{2\pi j^{n+1}} \frac{1}{\sqrt{2n(n+1)}} \\ &\quad \times \int_0^{2\pi} \int_{\pi/2+j\infty}^{\pi} \left[\begin{pmatrix} -m\pi_n^{(|m|)}(\beta_R) \\ \tau_n^{(|m|)}(\beta_R) \end{pmatrix} \mathbf{e}_{\beta_R} + j \begin{pmatrix} -\tau_n^{(|m|)}(\beta_R) \\ m\pi_n^{(|m|)}(\beta_R) \end{pmatrix} \mathbf{e}_{\alpha_R} \right] \\ &\quad \times e^{jm\alpha_R} e^{-2jk_s z_0 \cos \beta_R} e^{j\mathbf{k}_R(\beta_R, \alpha_R) \cdot \mathbf{r}} \sin \beta_R \, d\beta_R \, d\alpha_R. \end{aligned}$$

To compute $\mathbf{M}_{mn}^{3,R}$ and $\mathbf{N}_{mn}^{3,R}$ we introduce the image coordinate system $O'x'y'z'$ by shifting the original coordinate system a distance $2z_0$ along the positive z -axis. The geometry of the image coordinate system is shown in Fig. 4.3. Taking into account that $\mathbf{k}_R \cdot \mathbf{r}' = \mathbf{k}_R \cdot \mathbf{r} - 2k_s z_0 \cos \beta_R$, where $\mathbf{r}' = (x', y', z')$, we identify in the resulting equation the integral representations for the radiating vector

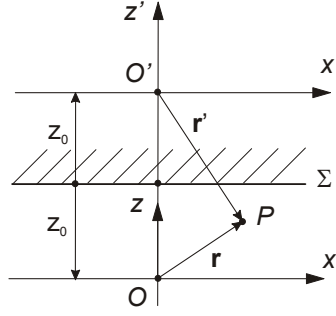


Fig. 4.3. Image coordinate system.

spherical wave functions in the half-space $z < 0$:

$$\begin{pmatrix} \mathbf{M}_{mn}^{3,\text{R}}(k_s \mathbf{r}) \\ \mathbf{N}_{mn}^{3,\text{R}}(k_s \mathbf{r}) \end{pmatrix} = (-1)^{n-|m|} r(0) \begin{pmatrix} -\mathbf{M}_{mn}^3(k_s \mathbf{r}') \\ \mathbf{N}_{mn}^3(k_s \mathbf{r}') \end{pmatrix}.$$

In this case the interacting field is the image of the scattered field and the expansion (4.6) can be derived by using the addition theorem for vector spherical wave functions. The elements of the reflection matrix are the translation coefficients, and as a result, the amount of computer time required to solve the scattering problem is significantly reduced. In this regard it should be mentioned that the formalism using the approximate expression for the reflection matrix has been employed by Videen [6–8].

In most practical situations we are interested in the analysis of the scattered field in the far-field region and below the plane surface, i.e., for $\theta > \pi/2$. In this region we have two contributions to the scattered field: the direct electric far-field pattern $\mathbf{E}_{s\infty}(\theta, \varphi)$,

$$\mathbf{E}_{s\infty}(\theta, \varphi) = \frac{1}{k_s} \sum_{n=1}^{\infty} \sum_{m=-n}^n (-j)^{n+1} [f_{mn} \mathbf{m}_{mn}(\theta, \varphi) + jg_{mn} \mathbf{n}_{mn}(\theta, \varphi)] \quad (4.17)$$

and the interacting electric far-field pattern $\mathbf{E}_{s\infty}^{\text{R}}(\theta, \varphi)$,

$$\mathbf{E}_{s\infty}^{\text{R}}(\theta, \varphi) = \frac{1}{k_s} \sum_{n=1}^{\infty} \sum_{m=-n}^n (-j)^{n+1} [f_{mn} \mathbf{m}_{mn}^{\text{R}}(\theta, \varphi) + jg_{mn} \mathbf{n}_{mn}^{\text{R}}(\theta, \varphi)], \quad (4.18)$$

where \mathbf{m}_{mn} and \mathbf{n}_{mn} are the vector spherical harmonics, and $\mathbf{m}_{mn}^{\text{R}}$ and $\mathbf{n}_{mn}^{\text{R}}$ are the reflected vector spherical harmonics,

$$\begin{aligned} \mathbf{m}_{mn}^{\text{R}}(\theta, \varphi) &= \frac{1}{\sqrt{2n(n+1)}} e^{-2jk_s z_0 \cos \theta} \\ &\times \left[jm\pi_n^{|m|}(\pi - \theta) r_{\parallel}(\pi - \theta) \mathbf{e}_{\theta} - \tau_n^{|m|}(\pi - \theta) r_{\perp}(\pi - \theta) \mathbf{e}_{\varphi} \right] e^{jm\varphi}, \end{aligned}$$

$$\mathbf{n}_{mn}^R(\theta, \varphi) = \frac{1}{\sqrt{2n(n+1)}} e^{-2jk_s z_0 \cos \theta} \\ \times \left[\tau_n^{|m|}(\pi - \theta) r_{\parallel}(\pi - \theta) \mathbf{e}_{\theta} + jm\pi_n^{|m|}(\pi - \theta) r_{\perp}(\pi - \theta) \mathbf{e}_{\varphi} \right] e^{jm\varphi}.$$

Thus, the solution of the scattering problem in the framework of the separation of variables method involves the following steps:

1. calculation of the \mathbf{T} -matrix relating the expansion coefficients of the fields striking the particle to the scattered field coefficients;
2. calculation of the reflection matrix \mathbf{A} characterizing the reflection of vector spherical wave functions by the surface;
3. computation of an approximate solution by solving the matrix equation (4.11);
4. computation of the far-field pattern by using (4.17) and (4.18).

In practice, we must compute the integrals in (4.13)–(4.16), which are of the form

$$I = \int_0^{\pi/2 - j\infty} f(\cos \beta) e^{2jq \cos \beta} \sin \beta \, d\beta.$$

Changing variables from β to $x = -2jq(\cos \beta - 1)$, we have

$$I = \frac{e^{2jq}}{2jq} \int_0^{\infty} f\left(1 - \frac{x}{2jq}\right) e^{-x} \, dx,$$

and integrals of this type can be computed efficiently by using the Laguerre polynomials [5].

Scanning near-field optical microscopy [18, 19] requires a rigorous analysis of the evanescent scattering by small particles near the surface of a dielectric prism [20–23]. The scattering of evanescent waves can be analyzed by extending our formalism to the case of an incident plane wave propagating in the substrate (Fig. 4.4).

For the incident vector plane wave given by (4.1), the transmitted (or the refracted) vector plane wave is

$$\mathbf{E}_{eT}(\mathbf{r}) = (E_{e0,\beta}^T \mathbf{e}_{\beta T} + E_{e0,\alpha}^T \mathbf{e}_{\alpha T}) e^{j\mathbf{k}_{eT} \cdot \mathbf{r}},$$

where

$$E_{e0,\beta}^T = t_{\parallel}(\beta_0) e^{jk_s z_0 (\cos \beta - m_{rs} \cos \beta_0)} E_{e0,\beta}, \\ E_{e0,\alpha}^T = t_{\perp}(\beta_0) e^{jk_s z_0 (\cos \beta - m_{rs} \cos \beta_0)} E_{e0,\alpha},$$

β_0 is the incident angle and $(\mathbf{e}_{kT}, \mathbf{e}_{\beta T}, \mathbf{e}_{\alpha T})$ are the spherical unit vectors of the transmitted wave vector \mathbf{k}_{eT} . The Fresnel transmission coefficients are given by

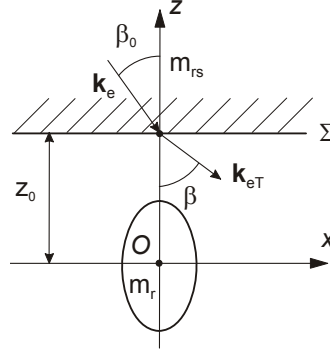


Fig. 4.4. Geometry of an axisymmetric particle situated near a plane surface. The external excitation is a vector plane wave propagating in the substrate.

$$t_{\parallel}(\beta_0) = \frac{2m_{rs} \cos \beta_0}{\cos \beta_0 + m_{rs} \cos \beta},$$

$$t_{\perp}(\beta_0) = \frac{2m_{rs} \cos \beta_0}{m_{rs} \cos \beta_0 + \cos \beta},$$

while the angle of refraction is computed by using Snell's law:

$$\sin \beta = m_{rs} \sin \beta_0,$$

$$\cos \beta = \pm \sqrt{1 - \sin^2 \beta}.$$

Evanescient waves appear for real m_{rs} and incident angles $\beta_0 > \beta_{0c}$, where $\beta_{0c} = \arcsin(1/m_{rs})$. In this case, $\sin \beta > 1$ and $\cos \beta$ is purely imaginary. For negative values of z , we have

$$\exp(j\mathbf{k}_{eT} \cdot \mathbf{r}) = \exp(-jk_s z \cos \beta + jk_s x \sin \beta) = \exp(jk_s |z| \cos \beta + jk_s x \sin \beta),$$

and we choose the sign of the square root such that $\text{Im}\{\cos \beta\} > 0$. This choice guarantees that the amplitude of the refracted wave propagating in the negative direction of the z -axis decreases with increasing the distance $|z|$. The expansion coefficients of the transmitted wave are

$$a_{mn_1}^T = -\frac{4j^{n_1}}{\sqrt{2n_1(n_1+1)}} \left[jm\pi_{n_1}^{|m|}(\pi - \beta) E_{e0,\beta}^T + \tau_{n_1}^{|m|}(\pi - \beta) E_{e0,\alpha}^T \right],$$

$$b_{mn_1}^T = -\frac{4j^{n_1+1}}{\sqrt{2n_1(n_1+1)}} \left[\tau_{n_1}^{|m|}(\pi - \beta) E_{e0,\beta}^T - jm\pi_{n_1}^{|m|}(\pi - \beta) E_{e0,\alpha}^T \right],$$

and we see that our previous analysis remains unchanged if we replace the total expansion coefficients a_{mn_1} and b_{mn_1} by the expansion coefficients of the transmitted wave $a_{mn_1}^T$ and $b_{mn_1}^T$.

4.1.2 Single particle on or near a plane surface coated with a film

The scattering by a particle situated on a plane surface coated with a film can be also treated with the above formalism. The major changes concern with the calculation of the Fresnel reflection coefficients which enter in the expression of the reflection matrix and the reflected incident field. To compute the Fresnel reflection coefficients we consider the scattering of a plane wave by a layered plane-parallel structure. The scattering geometry is shown in Fig. 4.5. The thickness of the film is d , while the relative refractive indices of the film and of the substrate are m_{rf} and m_{rs} , respectively. The electric fields in the three regions (ambient medium, film and substrate) are given by

$$\begin{aligned}\mathbf{E}(\mathbf{r}) &= (E_{\beta}\mathbf{e}_{\beta} + E_{\alpha}\mathbf{e}_{\alpha})e^{i\mathbf{k}_s\cdot\mathbf{r}} + (E_{\beta R}\mathbf{e}_{\beta R} + E_{\alpha R}\mathbf{e}_{\alpha R})e^{i\mathbf{k}_R\cdot\mathbf{r}}, \\ \mathbf{E}_f(\mathbf{r}) &= (E_{\beta T}\mathbf{e}_{\beta T} + E_{\alpha T}\mathbf{e}_{\alpha T})e^{i\mathbf{k}_T\cdot\mathbf{r}} + (E_{\beta fR}\mathbf{e}_{\beta fR} + E_{\alpha fR}\mathbf{e}_{\alpha fR})e^{i\mathbf{k}_{fR}\cdot\mathbf{r}}, \\ \mathbf{E}_s(\mathbf{r}) &= (E_{\beta fT}\mathbf{e}_{\beta fT} + E_{\alpha fT}\mathbf{e}_{\alpha fT})e^{i\mathbf{k}_{fT}\cdot\mathbf{r}},\end{aligned}$$

while the magnetic fields read as

$$\begin{aligned}\mathbf{H}(\mathbf{r}) &= (-E_{\alpha}\mathbf{e}_{\beta} + E_{\beta}\mathbf{e}_{\alpha})e^{i\mathbf{k}_s\cdot\mathbf{r}} + (-E_{\alpha R}\mathbf{e}_{\beta R} + E_{\beta R}\mathbf{e}_{\alpha R})e^{i\mathbf{k}_R\cdot\mathbf{r}}, \\ \mathbf{H}_f(\mathbf{r}) &= \sqrt{\varepsilon_{\text{rf}}}(-E_{\alpha T}\mathbf{e}_{\beta T} + E_{\beta T}\mathbf{e}_{\alpha T})e^{i\mathbf{k}_T\cdot\mathbf{r}} \\ &\quad + \sqrt{\varepsilon_{\text{rf}}}(-E_{\alpha fR}\mathbf{e}_{\beta fR} + E_{\beta fR}\mathbf{e}_{\alpha fR})e^{i\mathbf{k}_{fR}\cdot\mathbf{r}}, \\ \mathbf{H}_s(\mathbf{r}) &= \sqrt{\varepsilon_{\text{rs}}}(-E_{\alpha fT}\mathbf{e}_{\beta fT} + E_{\beta fT}\mathbf{e}_{\alpha fT})e^{i\mathbf{k}_{fT}\cdot\mathbf{r}}.\end{aligned}$$

The incident wave vector encloses the angle β_0 with the z -axis, and as a result, the wave vectors in the different regions can be expressed as.

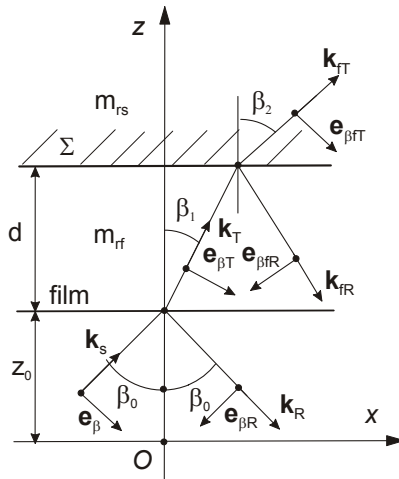


Fig. 4.5. Scattering geometry of a particle on a plane surface coated with a film.

$$\begin{aligned}
\mathbf{k}_s &= k_s (\sin \beta_0 \mathbf{e}_x + \cos \beta_0 \mathbf{e}_y), \\
\mathbf{k}_R &= k_s (\sin \beta_0 \mathbf{e}_x - \cos \beta_0 \mathbf{e}_y), \\
\mathbf{k}_T &= m_{\text{rf}} k_s (\sin \beta_1 \mathbf{e}_x + \cos \beta_1 \mathbf{e}_y), \\
\mathbf{k}_{\text{fR}} &= m_{\text{rf}} k_s (\sin \beta_1 \mathbf{e}_x - \cos \beta_1 \mathbf{e}_y), \\
\mathbf{k}_{\text{fT}} &= m_{\text{rs}} k_s (\sin \beta_2 \mathbf{e}_x + \cos \beta_2 \mathbf{e}_y).
\end{aligned}$$

The angles of incidence and refraction are related to each other by Snell's law:

$$\sin \beta_0 = m_{\text{rf}} \sin \beta_1 = m_{\text{rs}} \sin \beta_2,$$

and the cosine of the refraction angles are computed accordingly to the relations

$$\begin{aligned}
\cos \beta_1 &= \pm \sqrt{1 - \sin^2 \beta_1}, \quad \text{Im}(m_{\text{rf}} \cos \beta_1) > 0, \\
\cos \beta_2 &= \pm \sqrt{1 - \sin^2 \beta_2}, \quad \text{Im}(m_{\text{rs}} \cos \beta_2) > 0.
\end{aligned}$$

Imposing the boundary conditions at the interfaces between the regions

$$\mathbf{e}_z \times \mathbf{E}(\mathbf{r}) = \mathbf{e}_z \times \mathbf{E}_f(\mathbf{r}), \quad \mathbf{e}_z \times \mathbf{H}(\mathbf{r}) = \mathbf{e}_z \times \mathbf{H}_f(\mathbf{r}), \quad \mathbf{r} = z_0 \mathbf{e}_z$$

and

$$\mathbf{e}_z \times \mathbf{E}_f(\mathbf{r}) = \mathbf{e}_z \times \mathbf{E}_s(\mathbf{r}), \quad \mathbf{e}_z \times \mathbf{H}_f(\mathbf{r}) = \mathbf{e}_z \times \mathbf{H}_s(\mathbf{r}), \quad \mathbf{r} = (z_0 + d) \mathbf{e}_z$$

yields the desired relations

$$E_{\beta R} = r_{\perp}(\beta_0) E_{\beta}, \quad E_{\alpha R} = r_{\parallel}(\beta_0) E_{\alpha},$$

where the Fresnel reflection coefficients are now given by

$$\begin{aligned}
r_{\parallel}(\beta_0) &= \frac{r_{\parallel}^{01}(\beta_0) + r_{\parallel}^{12}(\beta_0) e^{2j m_{\text{rf}} k_s d \cos \beta_1}}{1 + r_{\parallel}^{01}(\beta_0) r_{\parallel}^{12}(\beta_0) e^{2j m_{\text{rf}} k_s d \cos \beta_1}} e^{2j k_s z_0 \cos \beta}, \\
r_{\perp}(\beta_0) &= \frac{r_{\perp}^{01}(\beta_0) + r_{\perp}^{12}(\beta_0) e^{2j m_{\text{rf}} k_s d \cos \beta_1}}{1 + r_{\perp}^{01}(\beta_0) r_{\perp}^{12}(\beta_0) e^{2j m_{\text{rf}} k_s d \cos \beta_1}} e^{2j k_s z_0 \cos \beta},
\end{aligned}$$

with

$$\begin{aligned}
r_{\parallel}^{01}(\beta_0) &= \frac{m_{\text{rf}} \cos \beta_0 - \cos \beta_1}{m_{\text{rf}} \cos \beta_0 + \cos \beta_1}, \\
r_{\perp}^{01}(\beta_0) &= \frac{\cos \beta_0 - m_{\text{rf}} \cos \beta_1}{\cos \beta_0 + m_{\text{rf}} \cos \beta_1}, \\
r_{\parallel}^{12}(\beta_0) &= \frac{m_{\text{rs}} \cos \beta_1 - m_{\text{rf}} \cos \beta_2}{m_{\text{rs}} \cos \beta_1 + m_{\text{rf}} \cos \beta_2}, \\
r_{\perp}^{12}(\beta_0) &= \frac{m_{\text{rf}} \cos \beta_1 - m_{\text{rs}} \cos \beta_2}{m_{\text{rf}} \cos \beta_1 + m_{\text{rs}} \cos \beta_2}.
\end{aligned}$$

It is apparent that when $d \rightarrow 0$, then

$$\frac{r_{\parallel}^{01}(\beta_0) + r_{\parallel}^{12}(\beta_0) e^{2jm_{\text{rf}}k_s d \cos \beta_1}}{1 + r_{\parallel}^{01}(\beta_0)r_{\parallel}^{12}(\beta_0) e^{2jm_{\text{rf}}k_s d \cos \beta_1}} \rightarrow \frac{m_{\text{rs}} \cos \beta_0 - \cos \beta_2}{m_{\text{rs}} \cos \beta_0 + \cos \beta_2} = r_{\parallel}^{02}(\beta_0)$$

and similarly,

$$\frac{r_{\perp}^{01}(\beta_0) + r_{\perp}^{12}(\beta_0) e^{2jm_{\text{rf}}k_s d \cos \beta_1}}{1 + r_{\perp}^{01}(\beta_0)r_{\perp}^{12}(\beta_0) e^{2jm_{\text{rf}}k_s d \cos \beta_1}} \rightarrow \frac{\cos \beta_0 - m_{\text{rs}} \cos \beta_1}{\cos \beta_0 + m_{\text{rs}} \cos \beta_1} = r_{\perp}^{02}(\beta_0).$$

In this case, the solution corresponds to a particle situated on the plane surface. For $m_{\text{rf}} = m_{\text{rs}}$, the identities $r_{\parallel}^{12}(\beta_0) = r_{\perp}^{12}(\beta_0) = 0$, imply that

$$r_{\parallel}(\beta_0) = r_{\parallel}^{01}(\beta_0) e^{2jk_s z_0 \cos \beta}, \quad r_{\perp}(\beta_0) = r_{\perp}^{01}(\beta_0) e^{2jk_s z_0 \cos \beta},$$

and we obtain the solution corresponding to a particle situated on the film. When the film is absorbing and $d \rightarrow \infty$, we see that

$$e^{2jm_{\text{rf}}k_s d \cos \beta_1} \rightarrow 0,$$

and as before, we obtain the solution corresponding to a particle situated on the film.

4.1.3 System of particles on or near a plane surface

To compute the scattering characteristics of a system of particles on a plane surface we have to account for the surface interaction among the particles. In the following analysis we follow the formulation presented by Mackowski [24] for sphere clusters on a plane interface.

The situation under examination is illustrated in Fig. 4.6. The system consists of \mathcal{N} particles each characterized by a position vector \mathbf{r}_{0i} , while the plane surface is placed at the distance z_0 with respect to the origin of a global coordinate system.

The field exciting the particle i consists of the direct and the reflected incident field and the contribution from the individual particles. This contribution includes the direct and the reflected components of the scattered field due to the particle j , and we have the representation

$$\mathbf{E}_{\text{exc},i}(\mathbf{r}_i) = \mathbf{E}_e(\mathbf{r}_i) + \mathbf{E}_e^{\text{R}}(\mathbf{r}_i) + \mathbf{E}_{\text{s},i}^{\text{R}}(\mathbf{r}_i) + \sum_{j \neq i}^{\mathcal{N}} \mathbf{E}_{\text{s},j}(\mathbf{r}_j) + \mathbf{E}_{\text{s},j}^{\text{R}}(\mathbf{r}_j).$$

The incident field is expressed in the global coordinate system

$$\mathbf{E}_e(\mathbf{r}) + \mathbf{E}_e^{\text{R}}(\mathbf{r}) = \sum_{m_1 n_1}^{\infty} a_{m_1 n_1} \mathbf{M}_{m_1 n_1}^1(k_s \mathbf{r}) + b_{m_1 n_1} \mathbf{N}_{m_1 n_1}^1(k_s \mathbf{r}),$$

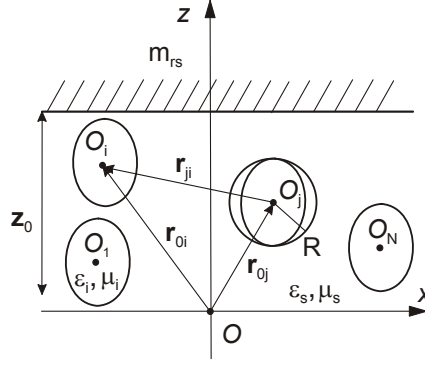


Fig. 4.6. Scattering geometry of a collection of particles on a plane surface.

whence using the addition theorem for regular spherical vector wave functions

$$\begin{bmatrix} \mathbf{M}_{m_1 n_1}^1(k_s \mathbf{r}) \\ \mathbf{N}_{m_1 n_1}^1(k_s \mathbf{r}) \end{bmatrix} = [\mathcal{T}_{m_1 n_1, mn}^{11}(k_s \mathbf{r}_{0i})] \begin{bmatrix} \mathbf{M}_{mn}^1(k_s \mathbf{r}_i) \\ \mathbf{N}_{mn}^1(k_s \mathbf{r}_i) \end{bmatrix},$$

yields a representation centered about the origin of the i th particle

$$\mathbf{E}_e(\mathbf{r}_i) + \mathbf{E}_e^R(\mathbf{r}_i) = \sum_{mn}^{\infty} a_{i,mn} \mathbf{M}_{mn}^1(k_s \mathbf{r}_i) + b_{i,mn} \mathbf{N}_{mn}^1(k_s \mathbf{r}_i)$$

with

$$\begin{bmatrix} a_{i,mn} \\ b_{i,mn} \end{bmatrix} = [\mathcal{T}_{m_1 n_1, mn}^{11}(k_s \mathbf{r}_{0i})] \begin{bmatrix} a_{m_1 n_1} \\ b_{m_1 n_1} \end{bmatrix}.$$

For the field scattered by the j th particle, we consider the series representation

$$\mathbf{E}_{s,j}(\mathbf{r}_j) = \sum_{m_1 n_1} f_{j,m_1 n_1} \mathbf{M}_{m_1 n_1}^3(k_s \mathbf{r}_j) + g_{j,m_1 n_1} \mathbf{N}_{m_1 n_1}^3(k_s \mathbf{r}_j),$$

and use the addition theorem

$$\begin{bmatrix} \mathbf{M}_{m_1 n_1}^3(k_s \mathbf{r}_j) \\ \mathbf{N}_{m_1 n_1}^3(k_s \mathbf{r}_j) \end{bmatrix} = [\mathcal{T}_{m_1 n_1, mn}^{31}(k_s \mathbf{r}_{ji})] \begin{bmatrix} \mathbf{M}_{mn}^1(k_s \mathbf{r}_i) \\ \mathbf{N}_{mn}^1(k_s \mathbf{r}_j) \end{bmatrix},$$

which is valid for $r_i < r_{ji}$, to derive

$$\mathbf{E}_{s,j}(\mathbf{r}_i) = \sum_{mn} f_{ij,mn} \mathbf{M}_{mn}^1(k_s \mathbf{r}_i) + g_{ij,mn} \mathbf{N}_{mn}^1(k_s \mathbf{r}_i),$$

with

$$\begin{bmatrix} f_{ij,mn} \\ g_{ij,mn} \end{bmatrix} = [\mathcal{T}_{m_1 n_1, mn}^{31}(k_s \mathbf{r}_{ji})] \begin{bmatrix} f_{j,m_1 n_1} \\ g_{j,m_1 n_1} \end{bmatrix}.$$

The reflected field scattered by the j th particle,

$$\mathbf{E}_{s,j}^R(\mathbf{r}_j) = \sum_{m_1 n_1} f_{j,m_1 n_1} \mathbf{M}_{m_1 n_1}^{3,R}(k_s \mathbf{r}_j) + g_{j,m_1 n_1} \mathbf{N}_{m_1 n_1}^{3,R}(k_s \mathbf{r}_j),$$

is first expressed in terms of regular spherical vector wave functions

$$\mathbf{E}_{s,j}^R(\mathbf{r}_j) = \sum_{m_2 n_2} f_{j,m_2 n_2}^R \mathbf{M}_{m_2 n_2}^1(k_s \mathbf{r}_j) + g_{j,m_2 n_2}^R \mathbf{N}_{m_2 n_2}^1(k_s \mathbf{r}_j),$$

where

$$\begin{bmatrix} f_{j,m_2 n_2}^R \\ g_{j,m_2 n_2}^R \end{bmatrix} = [A_{m_1 n_1, m_2 n_2}] \begin{bmatrix} f_{j,m_1 n_1} \\ g_{j,m_1 n_1} \end{bmatrix},$$

and A is the reflection matrix. Further using the transformation

$$\begin{bmatrix} \mathbf{M}_{m_2 n_2}^1(k_s \mathbf{r}_j) \\ \mathbf{N}_{m_2 n_2}^1(k_s \mathbf{r}_j) \end{bmatrix} = [\mathcal{T}_{m_2 n_2, mn}^{11}(k_s \mathbf{r}_{ji})] \begin{bmatrix} \mathbf{M}_{mn}^1(k_s \mathbf{r}_i) \\ \mathbf{N}_{mn}^1(k_s \mathbf{r}_j) \end{bmatrix},$$

we obtain a series representation centered about the origin of the i th particle, that is,

$$\mathbf{E}_{s,j}^R(\mathbf{r}_i) = \sum_{mn} f_{ij,mn}^R \mathbf{M}_{mn}^1(k_s \mathbf{r}_i) + g_{ij,mn}^R \mathbf{N}_{mn}^1(k_s \mathbf{r}_i),$$

with

$$\begin{bmatrix} f_{ij,mn}^R \\ g_{ij,mn}^R \end{bmatrix} = [\mathcal{T}_{m_2 n_2, mn}^{11}(k_s \mathbf{r}_{ji})] [A_{m_1 n_1, m_2 n_2}] \begin{bmatrix} f_{j,m_1 n_1} \\ g_{j,m_1 n_1} \end{bmatrix}.$$

Thus, the field exciting the i th particle can be expressed in terms of regular vector spherical wave functions centered at the origin O_i :

$$\mathbf{E}_{\text{exc},i}(\mathbf{r}_i) = \sum_{mn} \tilde{a}_{i,mn} \mathbf{M}_{mn}^1(k_s \mathbf{r}_i) + \tilde{b}_{i,mn} \mathbf{N}_{mn}^1(k_s \mathbf{r}_i),$$

with the expansion coefficients being given by

$$\begin{aligned} \begin{bmatrix} \tilde{a}_{i,mn} \\ \tilde{b}_{i,mn} \end{bmatrix} &= [\mathcal{T}_{m_1 n_1, mn}^{11}(k_s \mathbf{r}_{0i})] \begin{bmatrix} a_{m_1 n_1} \\ b_{m_1 n_1} \end{bmatrix} \\ &+ [A_{m_1 n_1, mn}] \begin{bmatrix} f_{i,m_1 n_1} \\ g_{i,m_1 n_1} \end{bmatrix} \\ &+ \sum_{j \neq i}^{\mathcal{N}} ([\mathcal{T}_{m_1 n_1, mn}^{31}(k_s \mathbf{r}_{ji})] + [\mathcal{T}_{m_2 n_2, mn}^{11}(k_s \mathbf{r}_{ji})] [A_{m_1 n_1, m_2 n_2}]) \\ &\times \begin{bmatrix} f_{j,m_1 n_1} \\ g_{j,m_1 n_1} \end{bmatrix}, \end{aligned}$$

Using the \mathbf{T} -matrix equation

$$\begin{bmatrix} f_{i,m'n'} \\ g_{i,m'n'} \end{bmatrix} = [T_{m'n', mn}] \begin{bmatrix} \tilde{a}_{i,mn} \\ \tilde{b}_{i,mn} \end{bmatrix}$$

we obtain the interaction equations as

$$\begin{aligned} & (\mathbf{I} - [T_{m'n',mn}] [A_{m'n',mn}]) \begin{bmatrix} f_{i,m'n'} \\ g_{i,m'n'} \end{bmatrix} \\ & - \sum_{j \neq i}^{\mathcal{N}} [T_{m'n',mn}] ([\mathcal{T}_{m_1 n_1, mn}^{31}(k_s \mathbf{r}_{ji})] + [\mathcal{T}_{m_2 n_2, mn}^{11}(k_s \mathbf{r}_{ji})] [A_{m_1 n_1, m_2 n_2}]) \\ & \times \begin{bmatrix} f_{j, m_1 n_1} \\ g_{j, m_1 n_1} \end{bmatrix} = [T_{m'n',mn}] [\mathcal{T}_{m_1 n_1, mn}^{11}(k_s \mathbf{r}_{0i})] \begin{bmatrix} a_{m_1 n_1} \\ b_{m_1 n_1} \end{bmatrix}. \end{aligned}$$

Ensembling the interaction equations for all particles into a global system of equations, and using a direct or an iterative solution method, yield the expression of the scattered field coefficients.

The scattered field will be the sum of the direct and the reflected scattered fields of all particles. In practice, we use the far-field representation of the field scattered by the i th particle in the direction $\mathbf{e}_r(\theta, \varphi)$,

$$\mathbf{E}_{s,i}(\mathbf{r}) = \frac{e^{jk_s r_i}}{r_i} \left\{ \mathbf{E}_{s\infty,i}(\mathbf{e}_r) + O\left(\frac{1}{r_i}\right) \right\}$$

and the approximation

$$\frac{e^{jk_s r_i}}{r_i} = \frac{e^{jk_s r} e^{-jk_s \mathbf{e}_r \cdot \mathbf{r}_{0i}}}{r} \left[1 + O\left(\frac{1}{r}\right) \right],$$

to define the angular-dependent vector of scattering coefficients

$$\begin{bmatrix} f_{mn}(\mathbf{e}_r) \\ g_{mn}(\mathbf{e}_r) \end{bmatrix} = \sum_{l=1}^{\mathcal{N}} e^{-jk_s \mathbf{e}_r \cdot \mathbf{r}_{0l}} \begin{bmatrix} f_{i,mn} \\ g_{i,mn} \end{bmatrix}.$$

To account of multiple scattering effects, we then consider the expressions of the direct and the interacting electric far-field patterns $\mathbf{E}_{s\infty}(\theta, \varphi)$ and $\mathbf{E}_{s\infty}^R(\theta, \varphi)$ as given by (4.17) and (4.18) respectively, but with the angular-dependent scattering coefficients $f_{mn}(\mathbf{e}_r)$ and $g_{mn}(\mathbf{e}_r)$, in place of the scattering coefficients f_{mn} and g_{mn} .

4.1.4 Numerical simulation

In this section we present scattering results for an axisymmetric particle situated on or near a plane surface. As reference we use a computer program based on the discrete sources method [12, 13].

Figs 4.7, 4.8 and 4.9 show the differential scattering cross-sections for Fe-, Si- and SiO-spheroids with semi-axes $a = 0.05 \mu\text{m}$ and $b = 0.025 \mu\text{m}$. The relative refractive indices are: $m_r = 1.35 + 1.97j$ for Fe, $m_r = 4.37 + 0.08j$ for Si, and $m_r = 1.67$ for SiO. The particles are situated on a silicon substrate, the wavelength of the incident radiation is $\lambda = 0.488 \mu\text{m}$, and the incident angle

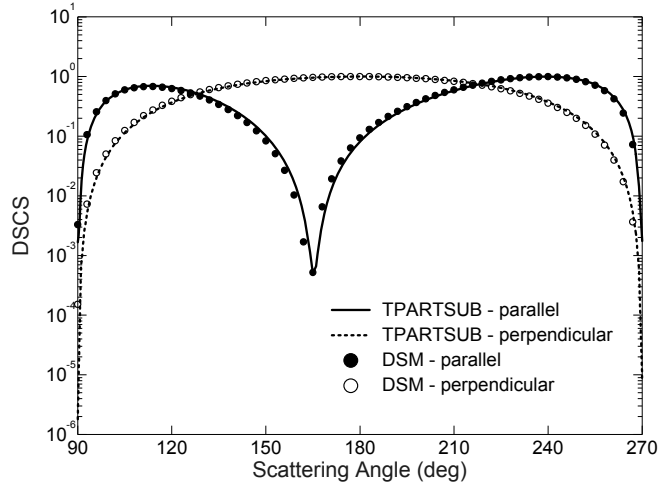


Fig. 4.7. Normalized differential scattering cross-sections of a Fe-spheroid computed with the TPARTSUB routine and the discrete sources method (DSM).

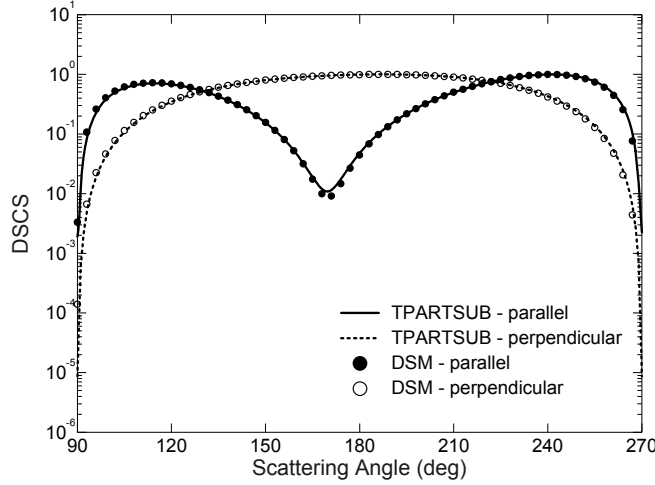


Fig. 4.8. Normalized differential scattering cross-sections of a Si-spheroid computed with the TPARTSUB routine and the discrete sources method (DSM).

is $\beta_0 = 45^\circ$. The plotted data show that the \mathbf{T} -matrix method leads to accurate results.

In the next example we investigate scattering of evanescent waves by particles situated on a glass prism. We note that evanescent wave scattering is important in various sensor applications such as the total internal reflection microscopy TIRM [25]. Choosing the wavelength of the external excitation as $\lambda = 0.488 \mu\text{m}$ and taking into account that the glass prism has a refractive index of $m_{\text{TS}} =$

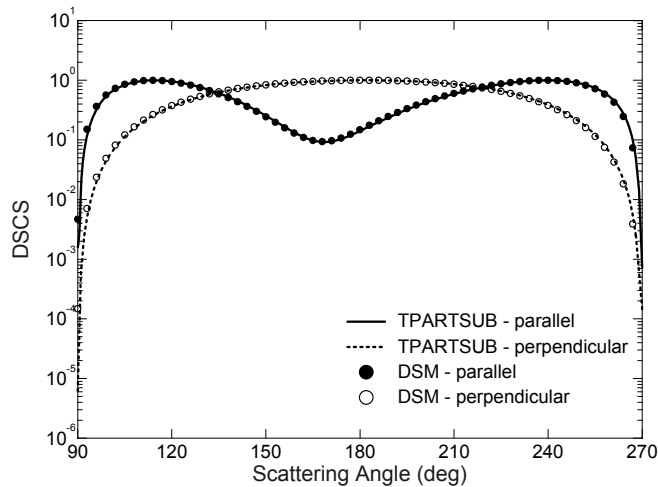


Fig. 4.9. Normalized differential scattering cross-sections of a SiO-spheroid computed with the TPARTSUB routine and the discrete sources method (DSM).

1.5, we deduce that the evanescent waves appear for incident angles exceeding 41.8° . In Figs. 4.10, 4.11 and 4.12 we plot the differential scattering cross-section for Ag-, diamond and Si-spheres with a diameter of $d = 0.2 \mu\text{m}$. The relative refractive indices of Ag- and diamond particles are $m_r = 0.25 + 3.14j$ and $m_r = 2.43$, respectively. The scattering plane coincides with the incident plane and the angle of incidence is $\beta_0 = 60^\circ$. The plotted data show a good agreement between the discrete sources and the \mathbf{T} -matrix solutions.

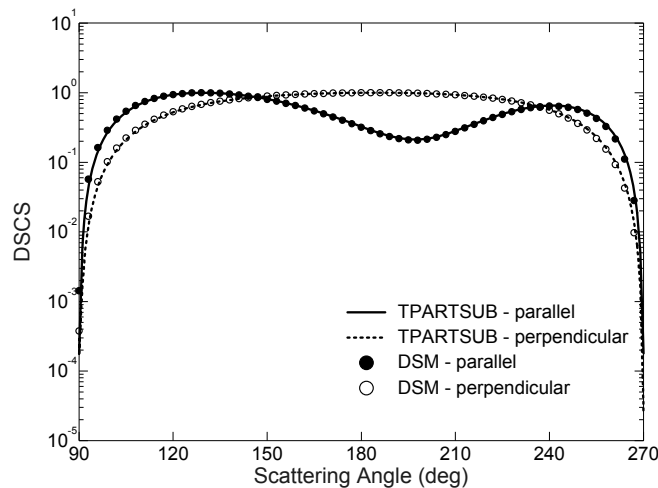


Fig. 4.10. Normalized differential scattering cross-sections of a metallic Ag-sphere computed with the TPARTSUB routine and the discrete sources method (DSM).

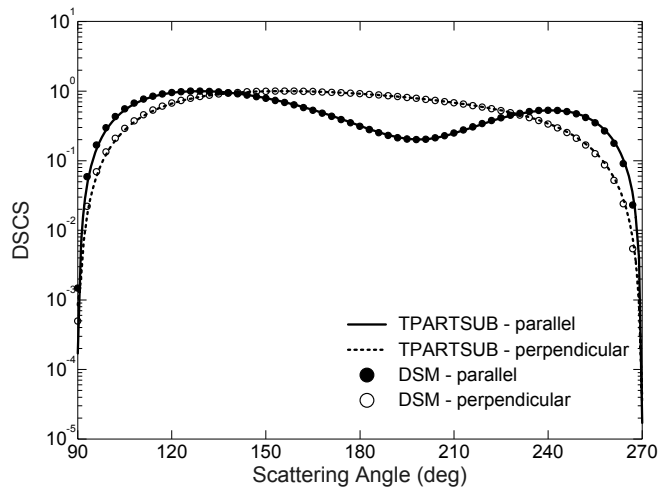


Fig. 4.11. Normalized differential scattering cross-sections of a Diamond-sphere computed with the TPARTSUB routine and the discrete sources method (DSM).

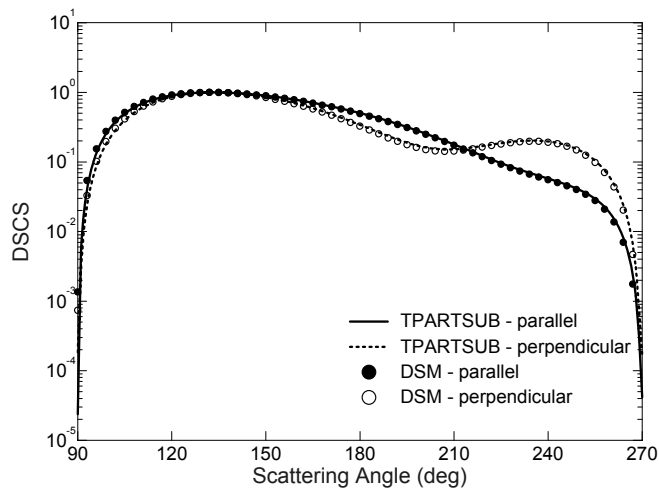


Fig. 4.12. Normalized differential scattering cross-sections of a Si-sphere computed with the TPARTSUB routine and the discrete sources method (DSM).

In Figs 4.13 and 4.14 we plot the differential scattering cross-sections for a spherical particle with radius $a = 0.05 \mu\text{m}$ situated on a plane surface coated with a film. The relative refractive indices are $m_r = 1.67$, $m_{rf} = 1.46 + 0.1j$ and $m_{rs} = 1.5$. The wavelength of the incident radiation is $\lambda = 0.488 \mu\text{m}$, and the incident angle is $\beta_0 = 45^\circ$. When the thickness d of the film is very small or

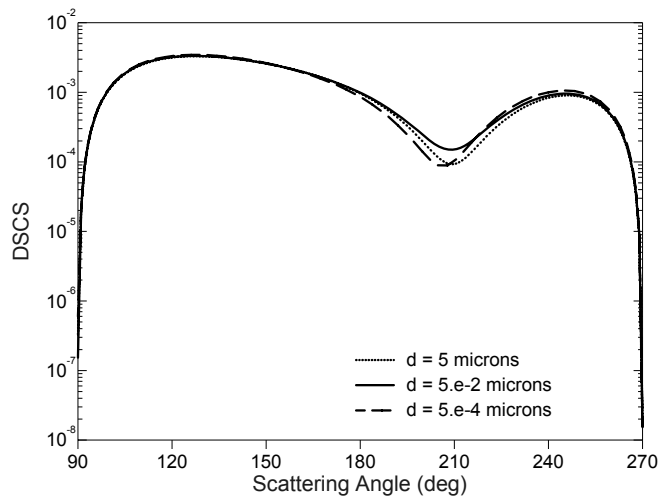


Fig. 4.13. Differential scattering cross-sections for parallel polarization of a spherical particle situated on a plane surface coated with a film.

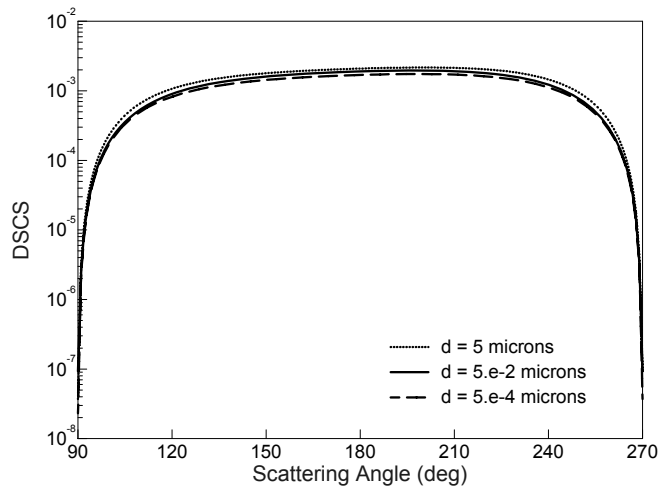


Fig. 4.14. Differential scattering cross-sections for perpendicular polarization of a spherical particle situated on a plane surface coated with a film.

very large, the differential scattering cross-sections correspond to the extreme situations of a particle situated on a plane surface with the refractive indices m_{TS} and m_{TF} , respectively.

The differential scattering cross-sections of two prolate spheroids with semi-axes $a = 0.1 \mu\text{m}$ and $b = 0.05 \mu\text{m}$ is shown in Fig. 4.15. Both particles are situated on the plane surface and the distance between their centers is $0.3 \mu\text{m}$. The relative refractive indices are $m_T = 1.5$ and $m_{TS} = 1.5$, while the wavelength

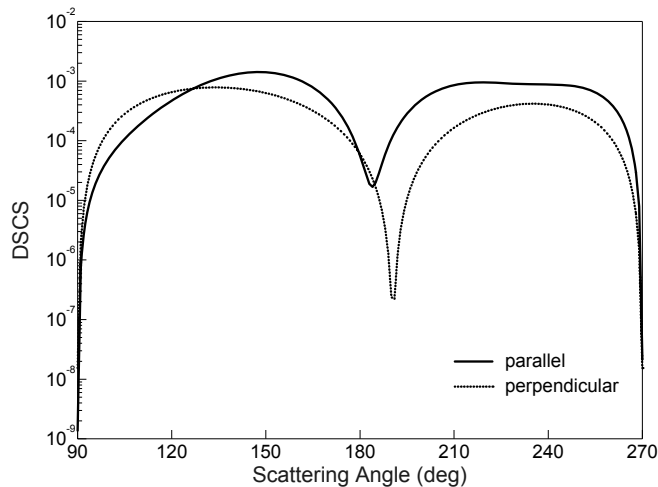


Fig. 4.15. Differential scattering cross-sections of two prolate spheroids situated on a plane surface

of the incident radiation and the incident angle are $\lambda = 0.628 \mu\text{m}$ and $\beta_0 = 45^\circ$, respectively

4.1.5 Conclusions

Relations for calculating the light-scattering from particles on or near a surface are provided. The formalism is based on the null-field method and the integral representation of vector spherical wave functions over plane waves. An approximate model is obtained as a special case by assuming that the scattered field reflecting off the surface and interacting with the particle is incident upon the surface at near-normal incidence. The formalism is of general use and can also be applied to the scattering of particles on a plane surface coated with a film and of a system of particles. The intention of this work has not been to comprehensively examine the scattering features of particles on plane surfaces. Rather, the objective has been to develop a formulation and a code which make tractable the exact calculations of such features.

Acknowledgement

We would like to acknowledge support of this research by DFG (Deutsche Forschungsgemeinschaft). We are especially grateful to Daniel Mackowski for providing the submitted version of his paper.

References

1. J. C. Stover: *Optical Scattering: Measurement and Analysis, 2nd edn* (SPIE Press, Bellingham, WA 1995).

2. B. Luk'yanchuk: *Laser Cleaning* (World Scientific, River Edge, NJ 2002).
3. S. Kawata, M. Ohtsu, M. Irie: *Near-Field Optics and Surface Plasmon Polaritons* (Springer, Berlin Heidelberg New York 2001).
4. A. Campion, P. Kambhampati: Surface-enhanced Raman scattering. *Chemical Society Reviews* **27**, 241 (1998).
5. P. A. Bobbert, J. Vlieger: Light scattering by a sphere on a substrate. *Physica* **137**, 209 (1986).
6. G. Videen: Light scattering from a sphere on or near a surface. *J. Opt. Soc. Am. A* **8**, 483 (1991).
7. G. Videen: Light scattering from a sphere behind a surface. *J. Opt. Soc. Am. A* **10**, 110 (1993).
8. G. Videen: Scattering from a small sphere near a surface. *J. Opt. Soc. Am. A* **10**, 118 (1993).
9. M. A. Taubenblatt, T. K. Tran: Calculation of light scattering from particles and structures on a surface by the coupled-dipole method. *J. Opt. Soc. Am. A* **10**, 912 (1993).
10. B. M. Nebeker, G. W. Starr, E. D. Hirleman: Light scattering from patterned surfaces and particles on surfaces. In *Optical Characterization Techniques for high Performance Microelectronic Device Manufacturing II*, ed. by J. K. Lowell, R. T. Chen, J. P. Mathur (Proc. SPIE **2638**, 1995), pp. 274–284.
11. R. Schmehl: The coupled-dipole method for light scattering from particles on plane surfaces. Diplomarbeit, Universität Karlsruhe (TH), Karlsruhe 1994.
12. Y. Eremin, N. Orlov: Simulation of light scattering from a particle upon a wafer surface. *Appl. Opt.* **35**, 6599 (1996).
13. Y. A. Eremin, N. V. Orlov: Analysis of light scattering by microparticles on the surface of a silicon wafer. *Optics and Spectroscopy* **82**, 434 (1997).
14. F. Moreno, F. Gonzalez: *Light Scattering from Microstructures* (Springer, Berlin 2000).
15. G. Kristensson, S. Ström: Scattering from buried inhomogeneities – a general three-dimensional formalism. *J. Acoust. Soc. Am.* **64**, 917 (1978).
16. R. H. Hackman, G. S. Sammelmann: Acoustic scattering in an homogeneous waveguide: Theory. *J. Acoust. Soc. Am.* **80**, 1447 (1986).
17. T. Wriedt, A. Doicu: Light scattering from a particle on or a near surface. *Opt. Commun.* **152**, 376 (1998).
18. R. C. Reddick, R. J. Warmack, T. L. Ferrell: New form of scanning optical microscopy. *Phys. Rev.* **39**, 767 (1989).
19. R. C. Reddick, R. J. Warmack, D. W. Chilcott, S. L. Sharp, T. L. Ferrell: Photon scanning tunneling microscopy. *Rev. Sci. Instrum.* **61**, 3669 (1990).
20. P. C. Chaumet, A. Rahmani, F. Fornel, J.-P. Dufour: Evanescent light scattering: The validity of the dipole approximation. *Phys. Rev.* **58**, 2310 (1998).
21. C. Liu, T. Kaiser, S. Lange, G. Schweiger: Structural resonances in a dielectric sphere illuminated by an evanescent wave. *Opt. Commun.* **117**, 521 (1995).
22. M. Quinten, A. Pack, R. Wannemacher: Scattering and extinction of evanescent waves by small particles. *Appl. Phys.* **68**, 87 (1999).
23. R. Wannemacher, A. Pack, M. Quinten: Resonant absorption and scattering in evanescent fields. *Appl. Phys.* **68**, 225 (1999).
24. D. Mackowski: Exact solution for the scattering and absorption properties of sphere clusters on a plane surface. JQSRT submitted.
25. D. C. Prieve: Measurement of colloidal forces with TIRM. *Advances in Colloid and Interface Science* **82**, 93 (1999).